# Multi Level Fusion of Competitive Sensors for Automotive Environment Perception

Mathias Haberjahn
Institute of
Transportation Systems
German Aerospace Center
12489 Berlin, Germany
Email: mathias.haberjahn@dlr.de

Karsten Kozempel
Institute of
Transportation Systems
German Aerospace Center
12489 Berlin, Germany
Email: karsten.kozempel@dlr.de

***Abstract*—A reference sensor system, consisting of a multilayer laser scanner and a stereo camera system, is used for detecting vehicle surroundings. Via a novel multi level multi sensor fusion framework the heterogeneous sensor information can be fused on three succeeding processing levels (low, mid and high level). Here the low level fusion achieved the highest accuracy in the description of the object hypotheses. Detection and processing faults can be recognized and reduced by competing sensor information within higher fusion levels. To combine the individual advantages and compensate for the disadvantages of the each level the different levels' results are merged in a V-shaped descent and ascent in the process chain. In the following the framework and the various methods for data fusion are presented and finally validated using real and simulated scenarios.**

## I. Introduction

More than three quarters of all traffic accidents in Germany are caused by drivers' mistakes [1]. A logical consequence to assist the human in the recognition and avoidance of dangerous situations, is the computer-based driver assistance. The sensor-based vehicle environment detection provides the basis for the automated driving assistance. The usage of homogeneous sensor networks often has a sensor-specific drawback. For instance, an image sensor needs an active light source and the field of view of a laser scanner is usually rather limited [2]. To avoid the sensor specific disadvantages of homogeneous sensors, the exploration and usage of heterogeneous sensors in the environment detection is increasing (see EU project Interactive [3]). Here, often one sensor is declared as the main sensor determining the object hypotheses and another one is only used for verification (for example radar and vision [4] or laser scanner and vision [5]). Missing detections by the main sensor remain undetected.

For reliable operation, the false positive and false negative rates have to be reduced and the accuracy of the object and situation determination must be increased. Reasons for the errors are the sensor specificity (e.g. negative environmental impacts on the measuring performance or accuracy), data processing (eg fragmentation and merging of object hypotheses, association errors) or the measurement conditions (e.g. occlusion).

The work ties in at this point and attempts to increase the vehicle environment perception in their reliability and accuracy by a competing fusion of heterogeneous sensor data at different levels of processing (fusion level). A fusion framework, developed for this purpose, allows the parallel or exclusive combination of the sensor data on the processing levels of spatial point information (low level), object data (mid level) and track data (high level). Contradictory sensor statements, based on a common sensing area, are used to identify missing and erroneous detections or processing errors of individual sensors by fusion on higher levels. Based on a reference sensor system, consisting of a multilayer laser scanner and a stereo camera, it is further shown that the data fusion at the lowest level, due to a high information density, provides the relatively most accurate object estimation. A combination all three levels' fusion results therefore reduces the measurement and processing errors and increases the accuracy of object determination.

The paper is structured as follows: Section II introduces the reference sensor used and the processing and fusion framework. The data fusion on the lower point level is described in section III while section IV focuses on the middle and higher object and track level fusion. In Section V the combination of the fusion levels is presented. Afterwards, the presented approaches are finally tested against ground truth and simulated data in section VI.

## II. Processing and Fusion Framework

### A. Reference Sensor

The sensor system consists of a 4-layer laser scanner (*IBEO - Lux*) and two side-mounted cameras (*Leutron Vision - PicSight*). The sensors are attached to the front of the measuring vehicle, sensing in driving direction. For further processing and recording the data is forwarded over an Ethernet interface into a vehicle-integrated computation unit. The acquisition timestamps of both sensors are hardware-synchronized in order to allow low level data fusion.

The parameters for mutual orientation and the systematic and random error of the sensors are determined in advance [6]. Therefore for each measurement point a model driven estimation of the measurement accuracy can be derived.

### B. Fusion Framework

The first systematic attempt to develop concepts for sensor data fusion in the automotive sector was in the EU project PReVENT ProFusion 1 and 2 [7]. The concepts developed

therein still represent the current state of the art in the following major automotive projects like interactIVe (2010 - 2013) [3], INTERSAFE-2 (2008 - 2011) [8] and HAVEit (2008 - 2011) [9].

Four essential fusion concepts were explored and listed in [7]:

- *Early Fusion*
- *Track-level Fusion*
- *Multi-level Fusion and Fusion Feedback*
- *Grid based Fusion*

The Multi-Level Multi-Sensor Fusion Framework (*MMFF*), presented here, can be considered as an extension to the Multi-level fusion formulated in [7] and [10]. The Multi-level fusion attempts to increase the accuracy of object determination by data fusion on the optimal fusion level depending on the included sensors and the specific application. A parallel level fusion for combining the level benefits, in contrast to the present work, does not take place. Another difference is the mutual independence of the embedded sensors and their processing in the MMFF to ensure an equal information competition. Thereby the MMFF is able to detect errors and false information by data fusion at higher processing levels.

As shown in figure 1, the spatial object points of the sensors are processed (fused) at the lowest level. Within the segmentation process the point information from different sensors is grouped independently or together into segments. On the mid level these segments are grouped and aligned to object hypotheses according to the real objects (*Merging / Shaping* [11]). The tempo-spatial movement of objects (*tracks*) is determined at the highest level within the tracking (*Extended Kalman Filter*). To obtain a joint track information the data from the two sensors can be fused at all three levels.

The framework is independent of the number and measuring method of included sensors, as long as the data (points, objects or tracks) and error models can be provided.

## III. Low Level Fusion

By data fusion at the lowest processing level (*LLF*) the measured point data from the sensors (3D Cartesian coordinates) is fused. For that the points are fed into a joint segmentation. This merging segmentation process does not differ from the single sensor segmentation. In order to make the segmentation independent from the sensor type, only the spatial information from the points is used discarding the image information from the stereo camera. Based on the segmentation approach described in [12] an additional sensor-specific segmentation model and an error model for the point information are taken into account.

The segmentation model defines the valid segmentation region of a sensor depending on the measuring principle, the measurement resolution and the distance and direction between measuring point and sensor. The segmentation region is denoted by the space around a certain point in which another point is probably mapping the same real object (*S-Ellipsoid* see figure 2(a)). The local segmentation behavior of a sensor can

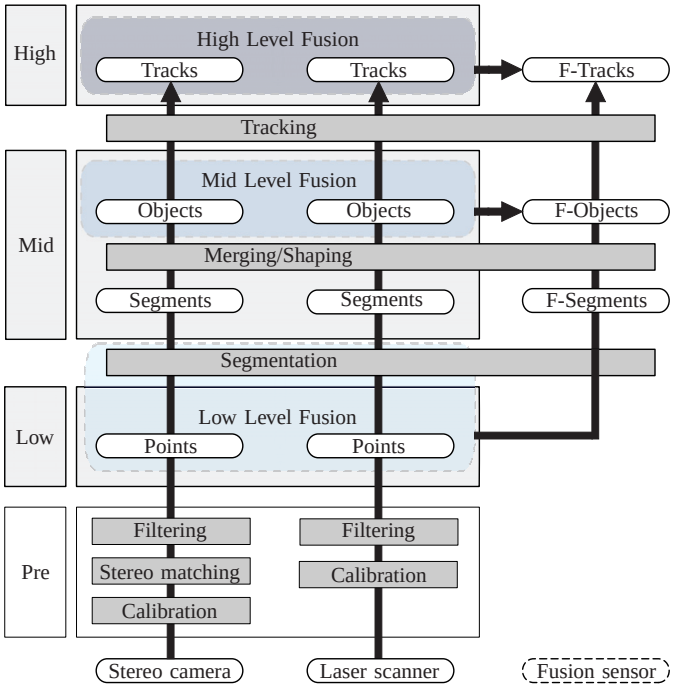


Fig. 1: Multi Level Multi Sensor Fusion framework for reference sensor system

be described by an appropriate choice of the distance factor $S$, a constant offset $O$ and an exponent $E$. Depending on the measurement distance $d$ the S-Ellipsoid is described with:

$$\begin{aligned} \mathcal{S}_a &= O_x + (S_x d)^{E_x} \\ \mathcal{S}_b &= O_y + (S_y d)^{E_y} \\ \mathcal{S}_c &= O_z + (S_z d)^{E_z} \ . \end{aligned} \tag{1}$$

The error model, however, defines the space around each measurement point (*F-Ellipsoid*), in which the true position of the point is located with a required probability $p$:

$$\begin{aligned} \mathcal{F}_a &= \Phi^{-1}\left(\frac{p+1}{2}\right)\sigma_x + \mu_x \\ \mathcal{F}_b &= \Phi^{-1}\left(\frac{p+1}{2}\right)\sigma_y + \mu_y \\ \mathcal{F}_c &= \Phi^{-1}\left(\frac{p+1}{2}\right)\sigma_z + \mu_z, \text{ with } \mu_x = \mu_y = \mu_z = 0 \ . \end{aligned} \tag{2}$$

As shown in figure 2(b) two points $P_1$ and $P_2$ are associated with the same segment if at least one F-Ellipsoid of one point encloses the S-ellipsoid of the other one completely [13].

For the LLF presented here the input point data from the sensors has to be acquired synchronously and in a common coordinate system. Figure 3 shows the LLF results for an exemplary traffic scene.

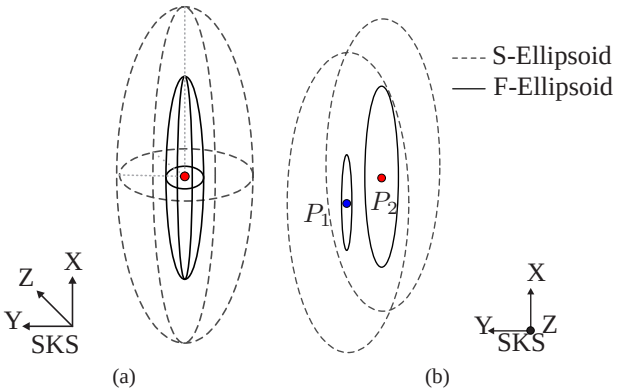


Fig. 2: S- and F-Ellipsoid for a measurement point $P_1$ (a); valid segmentation of two points according to their S- and F-Ellipsoid (2D view) (b)

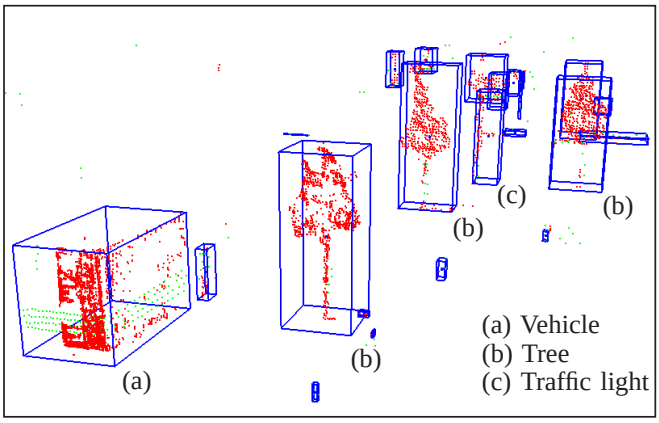


Fig. 3: Low Level Fusion by joint segmentation of the red dotted stereo and green dotted laser data

### A. Segmentation Probability

The segmentation probability $P(S_P^X)$ (*SP*) defines the probability for a valid segmentation $S$ for an existing object $O$ at the measurement point $P$ for a sensor $X$. For every point $P$ in the sensing area such a probability $P(S_P^X)$ can be estimated.

The horizontal SP is determined on the shortest distance $\bar{d}$ between the F-Ellipsoid $\mathcal{F}^{\bar{P}}$ of the horizontal neighbor $\bar{P}$ and the S-Ellipsoid $\mathcal{S}^P$ of $P$ (see figure 4) and the standard deviation $\bar{\sigma}$ of $\bar{P}$ with:

$$P(\bar{S}_P^X) = \begin{cases} \Phi\left(\frac{\bar{d}}{\bar{\sigma}}\right) & \text{, with } \bar{d} \geq 0 \\ 1 - \Phi\left(-\frac{\bar{d}}{\bar{\sigma}}\right) & \text{, with } \bar{d} < 0 \end{cases} \tag{3}$$

The shortest distance $\bar{d}$ equals the minimum of $\bar{d_x}$, $\bar{d_y}$ and $\bar{d_z}$. This distances are derived from the location of the F-Ellipsoid $\mathcal{F}^{\bar{P}}$ of the horizontal neighbor $\bar{P}$ within the S-Ellipsoid $\mathcal{S}^P$ of $P$:

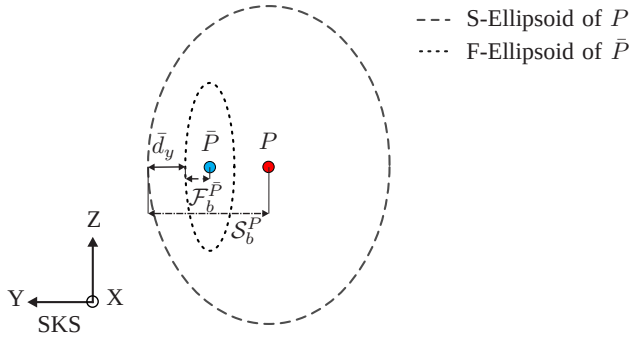


Fig. 4: Illustration of the distance $\bar{d}_y$ in Y-Direction between the S-Ellipsoid $\mathcal{S}_b^P$ of $P$ and the F-Ellipsoid $\mathcal{F}_b^{\bar{P}}$ of $\bar{P}$ for determination of the horizontal SP $P(\bar{S}_P)$ in $P$

$$\begin{aligned} \bar{d}_x &= \mathcal{S}_a^P - (\bar{P}_x + \mathcal{F}_a^{\bar{P}} - P_x) \\ \bar{d}_y &= \mathcal{S}_b^P - (\bar{P}_y + \mathcal{F}_b^{\bar{P}} - P_y) \\ \bar{d}_z &= \mathcal{S}_c^P - (\bar{P}_z + \mathcal{F}_c^{\bar{P}} - P_z) \end{aligned} \tag{4}$$

In the same way the vertical distance $\bar{\bar{d}}$ to the F-Ellipsoid $\mathcal{F}^{\bar{\bar{P}}}$ of $\bar{\bar{P}}$ and the vertical SP $P(\bar{\bar{S}}_P^X)$ are estimated. The total SP $P(S_P^X)$ at $P$ is set to the minimum of $P(\bar{S}_P^X)$ and $P(\bar{\bar{S}}_P^X)$.

## IV. Mid And High Level Fusion

In the Mid Level Fusion (*MLF*) object hypotheses of different sensors and in the High Level Fusion (*HLF*) object tracks are fused. In the following, the particular fusion steps are described.

### A. Mid Level Fusion

For the object data fusion, called mid-level fusion, the incoming object hypotheses are determined either directly in the sensor or in a subsequent processing unit. As a result a new object hypothesis is generated by a weighted fusion of the incoming objects from the involved sensors. At first all corresponding objects mapping the same real object are associated with each other within a clustering. Based on contradictory sensor assignments within the object clusters segmentation errors can be detected. As shown in figure 5 the segmentation errors are divided into fragmentation objects (*FO*), merging objects (*MO*), missing objects (*FNO*) and false objects (*FPO*) similar to [14]. Afterwards the error cleaned object clusters are fused by a *Simple Convex Combination* algorithm [11].

*Fragmentation and Merging Objects:* If not all involved sensors are able to associate an object to a certain cluster a segmentation error is presumed. In this case this conflict cluster $C_1$ is tested on the complementary effects object fragmentation and merging. This occurs if some object hypotheses of a second cluster $C_2$ overlapping $C_1$. The complementary probabilities for an FO $P(F^+)$ and MO $P(F^+)$ are determined depending on the degree of splitting or overlapping between the single object hypotheses and the cluster centers of $C_1$ and $C_2$. This is described by an overlapping $d_{F^+}$ and splitting

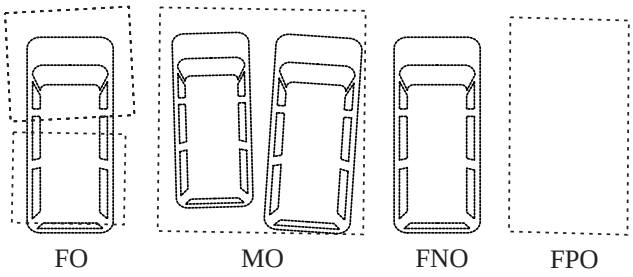


Fig. 5: Errors in segmentation: Fragmentation object (FO), merging object (MO), missing object (FNO) and false object (FPO)

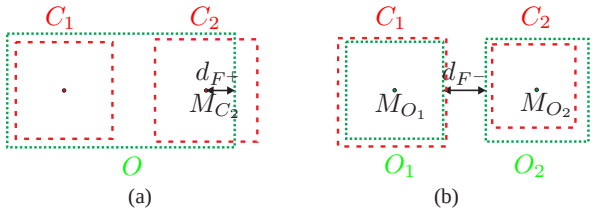


Fig. 6: Determination of overlapping distance $d_{F^+}$ between Object $O$ and cluster $C_2$ (a); Determination of splitting distance $d_{F^-}$ between Objects $O_1$ and $O_2$ (b)

distance $d_{F^-}$ and the accuracy of the clusters $\sigma_{M_C}$ and the objects $\sigma_{M_O}$ (see figure 6).

The so called overlapping probability $P^-(F_+)$ is determined by

$$P^-(F_+) = \begin{cases} \Phi\left(\frac{d_{F_+}}{\sigma_{M_C}}\right) & \text{, with } d_{F_+} \geq 0 \\ 1 - \Phi\left(-\frac{d_{F_+}}{\sigma_{M_C}}\right) & \text{, with } d_{F_+} < 0 \end{cases} \tag{5}$$

and together with the segmentation probability $P(S^X_{M_O})$ at $M_O$ the probability for an FO $P(F_+)$ is derived by

$$P(F_+) = (P^-(F_+) - \frac{1}{2})(\frac{3}{2} - P(S^X_{M_O})) + \frac{1}{2}\,. \tag{6}$$

In the same way the splitting probability $P^-(F_-)$ is determined by

$$P^-(F_-) = \begin{cases} \Phi\left(\frac{d_{F_-}}{\sigma_{M_O}}\right) & \text{, with } d_{F_-} \geq 0 \\ 1 - \Phi\left(-\frac{d_{F_-}}{\sigma_{M_O}}\right) & \text{, with } d_{F_-} < 0 \end{cases} \tag{7}$$

and

$$P(F_-) = (P^-(F_-) - \frac{1}{2})(P(S^Y_{M_{O_1O_2}})) + \frac{1}{2}\,. \tag{8}$$

The complementary probabilities $P(F_+)$ and $P(F_-)$ can be determined for each involved sensor for the two conflict clusters $C_1$ and $C_2$. To resolve this conflict the two probabilities are multiplied and compared:

$$\begin{aligned} \prod_{i=1}^{M} P_{X_i}(F_+) &> \prod_{i=1}^{M} P_{X_i}(F_-)\,, \text{ with } X^i \in (\mathbb{U} \cup \bar{\mathbb{U}}) \rightarrow \text{FO} \\ \prod_{i=1}^{M} P_{X_i}(F_+) &< \prod_{i=1}^{M} P_{X_i}(F_-)\,, \text{ with } X^i \in (\mathbb{U} \cup \bar{\mathbb{U}}) \rightarrow \text{MO} \\ \prod_{i=1}^{M} P_{X_i}(F_+) &= \prod_{i=1}^{M} P_{X_i}(F_-)\,, \text{ with } X^i \in (\mathbb{U} \cup \bar{\mathbb{U}}) \rightarrow \text{ND} \end{aligned} \tag{9}$$

In case of equality no decision can be taken (ND).

*Missing and False Objects:* If no other clusters overlap a conflict cluster $C_1$ a missing (FNO) or false detected object (FPO) is assumed. To solve the conflict for all involved sensors of $C_1$ the compound probabilities $P(E^+|D^+)$ and $P(E^-|D^+)$ have to be estimated. $P(E^+|D^+)$ equals the probability given an object hypothesis was detected $D^+$, the object exists in real $E^+$ and $P(E^-|D^+)$ the probability given an object hypothesis was detected $D^+$, the object does not exist $E^-$. Since these probabilities are not directly measurable, they are derived according to the *Bayes'* theorem from the likelihoods $P(D^+|E^+)$ and $P(D^+|E^-)$ and the prior probability $P(E^+)$. The likelihood is substituted by the analytically determined segmentation probability. For the $N$ involved sensors the two likelihoods can be fused by the *independent likelihood pool* [15]:

$$\begin{aligned} P(E_+|D^1_+, D^2_+, \ldots, D^N_+) &= \frac{P(D^1_+, D^2_+, \ldots, D^N_+|E_+)P(E_+)}{P(D^1_+, D^2_+, \ldots, D^N_+)} \\ P(E_-|D^1_+, D^2_+, \ldots, D^N_+) &= \frac{P(D^1_+, D^2_+, \ldots, D^N_+|E_-)P(E_-)}{P(D^1_+, D^2_+, \ldots, D^N_+)}\,. \end{aligned} \tag{10}$$

The maximum of the two posteriori probabilities $P(E_+|D^1_+, D^2_+, \ldots, D^N_+)$ and $P(E_-|D^1_+, D^2_+, \ldots, D^N_+)$ resolves the conflict between a missing or false object detection:

$$\begin{aligned} P(E_+|D^1_+, D^2_+, \ldots, D^N_+) &> P(E_-|D^1_+, D^2_+, \ldots, D^N_+) \rightarrow \text{FNO} \\ P(E_+|D^1_+, D^2_+, \ldots, D^N_+) &< P(E_-|D^1_+, D^2_+, \ldots, D^N_+) \rightarrow \text{FPO} \\ P(E_+|D^1_+, D^2_+, \ldots, D^N_+) &= P(E_-|D^1_+, D^2_+, \ldots, D^N_+) \rightarrow \text{ND} \end{aligned} \tag{11}$$

Again, in case of equality no decision can be taken (ND). An exemplary illustration of the MLF for a traffic scene is shown in figure 7.

### B. High Level Fusion

The sensors' single tracks representing the same object are fused into a system track in the HLF. Similar to the MLF the detected tracks from different sensors have to be associated to each other first. The clustering is basically an extension of

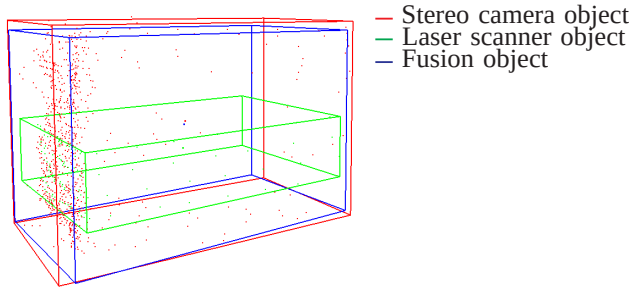


Fig. 7: Fusion object (blue) resulting from Mid Level Fusion of real stereo (red) and laser object data (green)

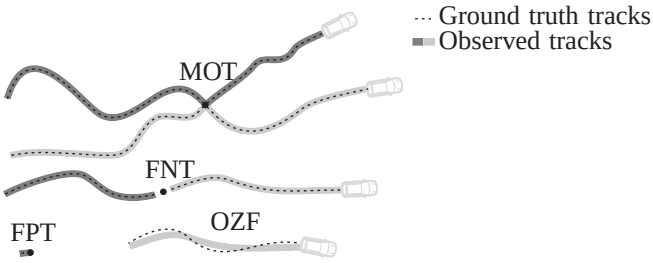


Fig. 8: Categorization of tracking errors into multi object Track (MOT), missing track (FNT), false track (FPT) and uncertainty of object state (OZF)

the MLF clustering. Besides the actual object state, the history states are taken into account to support a correct association. The incomplete cluster configurations are rated as an indicator for tracking errors as well. For that the clustering history of a system track is stored in a system cluster (see figure 9).

*Tracking Errors:* The tracking errors are separated into multi object track (*MOT*) (multiple tracked real objects per track) as well as missing track (*FNT*) and false track (*FPT*) (see figure 8).

The FPT/FNT effect is recognized within the system cluster by contradictory sensor statements regarding to missing object assignments. Figure 9 shows how sensor 3 missed to assign objects to the system cluster for the last three time steps (green framed). To solve the complementary FPT/FNT effect, the FPO/FNO approach from the MLF was extended by taking the track state accuracies into account.

The MOT effect, which results from a falsely changed tracking object within a track, can also be detected with the system cluster. As shown in figure 9 the red framed area shows a change of track id 3 to 4 for sensor 1. As a consequence the

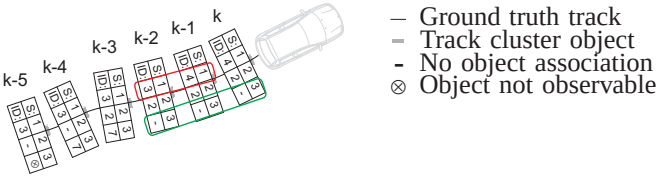


Fig. 9: System cluster of a system track with recognized FNT/FPT (green) and MOT effect (red)

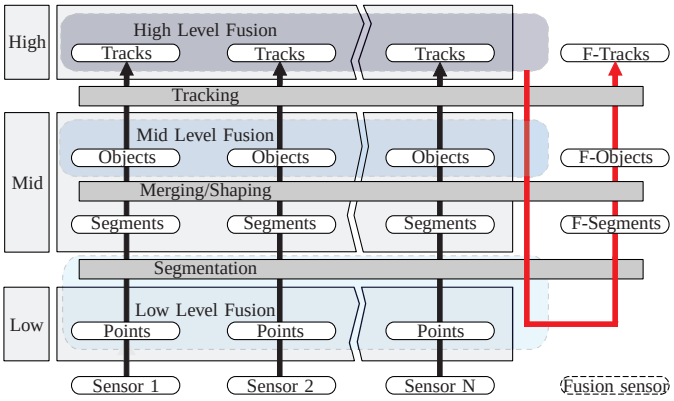


Fig. 10: Sequential combination of fusion levels

two wrong tracks are removed from the track cluster.

*State Fusion:* After cleaning the track clusters all tracks of one cluster are fused to obtain the system track. To filter the shared information within a track (*inter-track correlation*) and between tracks (*intra-track correlation*) and to avoid a distortion of the fusion weight, various methods have been developed. In this work three different track-to-track fusion approaches, the *Simple Convex Fusion* [16], [17], the *Fast Covariance Intersection Fusion* [18] and the *Information Fusion* [19], were tested and compared.

## V. Multi Level Fusion

Looking back on the advantages and disadvantages of the three fusion levels, it can be stated that with an increasing data processing, the accuracy of the object determination is decreasing. On the other side errors made in lower process steps can be caught at higher processing steps. The logical consequence is the bundling of the specific advantages of the three fusion levels with a sequential combination of the fusion methods.

In the sense of a descent, the object data, which was obtained by fusion of the upper processing levels, is mapped on the lower point level to get an optimum description of the object information by a following ascent in the process chain (see red arrow in figure 10).

Therefore the sensor data, taken from one time step, is fused independently on mid and high level. Afterwards the actual track states are mapped from the high on the object hypotheses of the mid level. Thus detected conflicts on higher level can confirmed or rejected by comparing them with the results of the mid level conflict detection. Then the cleaned object hypotheses are mapped into the point space of the sensors' on lower level. For every object $\check{O}$ a local segmentation is executed to get an optimal object description $\hat{O}$. Due to the imprecise high level object description the object box dimensions are doubled to specify the local segmentation area. In table I the actions for the prevention of tracking and segmentation errors in the local segmentation for an object $\check{O}$ are listed.

Those newly determined objects have the high description accuracy of the LLF and should be cleaned of detection and

| Error Type | Action for Avoidance |
|---|---|
| False detection (FPO, FPT) | No further action necessary, as false object and track hypotheses are already removed out of the hypotheses list by MLF and HLF |
| Missing detection (FNO, FNT) | No further action necessary, as missing detections are compensated by object detections from other sensors |
| Merging object (MO) | In case of a detected object merging (MO) for the corresponding cluster of $\tilde{O}$ only point sets from sensors, which are checked as correct detecting, are involved in the segmentation |
| Fragmentation object (FO) | In case of a detected object fragmentation (FO) for the corresponding cluster of $\tilde{O}$ no further actions are necessary, as a fragmentation is avoided by points sets of further sensors at the location of $\tilde{O}$ |

TABLE I: Actions for error avoidance in the local segmentation

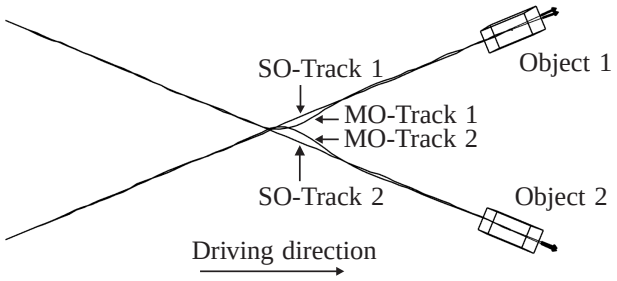


Fig. 11: Szenario 1: Two objects are crossing at an angle of $45^\circ$ with 50 km/h; Sensor 1 detects two error-free SOT's und Sensor 2 detects two faulty MOT's

processing errors by solving the conflicting sensor statements. The renewed objects pass the process chain again and get tracked. Here the error-prone object-to-track association can be dropped since the track id is already known from the descent.

## VI. Experimental Validation

The presented methods for data fusion are tested either by simulation or in real test scenarios. The results for the experimental validation of MOT detection and object state determination are listed below. For further experimental evaluations see [20].

### A. MOT Detection

The introduced detection approach of multi object tracks was tested in a simulation. In the simulated scenario two objects are crossing at an angle of $45^\circ$ with a constant speed of 50 km/h (see figure 11). One correct detecting sensor $S_1$ is tracking exactly one real object per track (single object track – *SOT*). A second sensor $S_2$ falsely switches the real objects and their tracks at the crossing point (multi object track). Each sensor is either detecting two SOT's or two MOT's.

The aim of the simulation was to determine the MOT causing sensor by evaluating the system cluster. Therefore the object positions were noised with normally distributed random values to analyze the dependence between MOT determination and measurement accuracy.

In table II the ratios between correctly detected MOT's and the total number of simulation steps depending on the sensor accuracy are listed. Every single simulation is repeated 1000 times. If the accuracy of both sensors is equal the MOT detection rate is over 89 %. This surprisingly high rate is due to the behavior of the MOT compared to SOT. The sudden difference between predicted an measured moving direction for a MOT leads to increasing track variances. This benefits the SOT within a correct system cluster creation. On the other hand the MOT detecting sensor is trusted more, in case it is more accurate than the SOT detecting one, which results in a falsely recognized MOT. Simulations with a second scenario and more than two involved sensors led to similar results.

| | SOT $\sigma$=0.01 m | SOT $\sigma$=0.1 m | SOT $\sigma$=0.2 m |
|---|---|---|---|
| MOT $\sigma$=0.01 m | 100 % | 0 % | 0 % |
| MOT $\sigma$=0.1 m | 100 % | 97.6 % | 0 % |
| MOT $\sigma$=0.2 m | 100 % | 100 % | 89.3 % |

TABLE II: Simulation of the MOT error detection for one true and one false tracking sensor with different measurement accuracies

### B. Accuracy Object Determination

To determine the accuracy of the object box description under real conditions, depending on the used fusion level, a second car was used as a reference vehicle $V_R$. The reference vehicle was equipped with two high-accuracy RTK capable GPS receivers. With knowledge of the vehicle dimensions and the gps positions a ground truth box of $V_R$ could be estimated in the UTM coordinate system.

The following analysis is based on a circular course driven by $V_R$ with about 11 rounds and 4063 individual measurement time steps. The circle center was about 35 meters located from the sensors, with an average radius of about 6 m.

The figures 12 to 13 show the overlap between the measurement and reference object box during the circular drive in percent. It can be seen that the stereo system provides a better covering (shown in red) compared to the laser scanner (green), which can be explained by the better height resolution of the stereo system (see figure 12).

As expected, in a direct comparison of the three fusion Levels the LLF (light blue) has the smallest error in the object description (see figure 13). MLF and HLF achieve a comparable accuracy, which is lying between the accuracies of the non-fused sensor data. The LLF outperforms even the individual sensors regarding the object estimation accuracy. In this comparison the Simple Convex Fusion was chosen for the HLF due to the best object estimation compared to the Information and Fast Covariance Intersection Fusion.

## VII. Conclusion

A novel, multi-level sensor fusion architecture was introduced, which reduces measurement and processing errors by a competing fusion on higher level and increases the accuracy and reliability of the sensor-based vehicle detection environment. Additionally the fusion framework is independent concerning the sensor number and measurement principle.

The comparatively best accuracy in the object description can be achieved by LLF. This was proved with real measurement data from the reference system, consisting of a laser

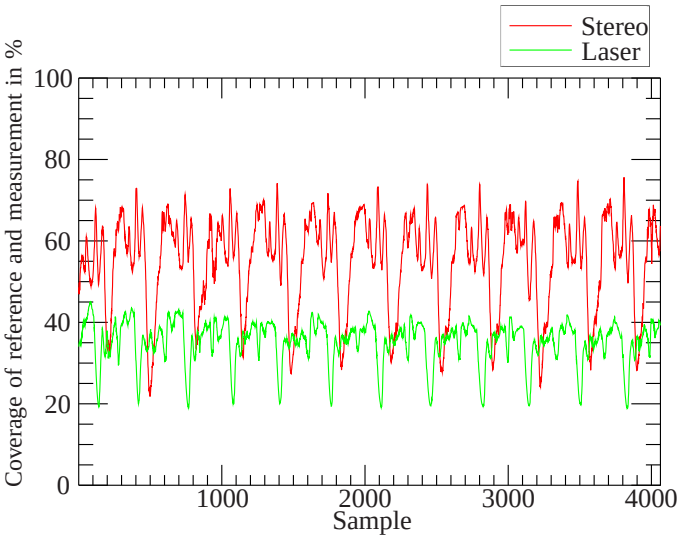


Fig. 12: Percentage coverage of the object volumes between tracked measurement objects of the sensors and the reference objects

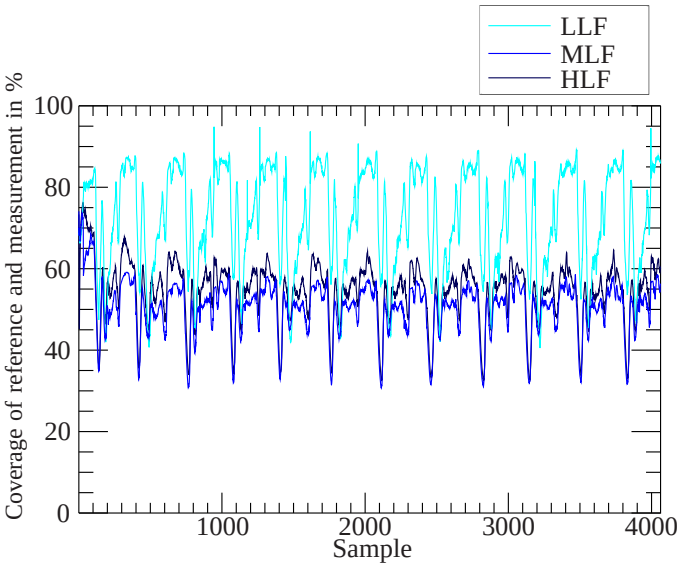


Fig. 13: Percentage coverage of the object volumes between tracked measurement objects of *LLF*, *MLF* und *HLF-SCF* and reference objects

scanner and a stereo camera. The efficiency of the MOT detection was shown by simulation.

## REFERENCES


[1] Statistisches Bundesamt, *Verkehr - Verkehrsunflle*, fachserie 8 reihe 7 ed., Statistisches Bundesamt, Wiesbaden, 2011.

[2] K. C. Fuerstenberg and K. Dietmayer, "Pedestrian recognition and tracking of vehicles using a vehicle based multilayer laserscanner," in *10th World Congress on Intelligent Transport Systems*, 2003.

[3] A. Amditis and U. Iurgel, "From fusion to perception : The perception subproject of interactive," in *8th ITS European Congress Lyon*, 2011.

[4] G. Allesandretti, A. Broggi, and P. Cerri, "Vehicle and guard rail detection using radar and vision data fusion," in *IEEE Transactions on Intelligent Transportation Systems*, vol. 8, no. 1, March 2007, pp. 95–105.

[5] S. Wender and K. Dietmayer, "3d vehicle detection using a laser scanner and a video camera," in *6th European Congress on ITS*, Aalborg, 2007.

[6] M. Haberjahn and R. Reulke, "Cross-kalibrierung eines mehrzeilen-laserscanner- und stereokamera-systems zur fahrzeugumfelderfassung," in *Proc. of 3D-Nordost*, no. 12, Berlin, 10-11 December 2009, pp. 119–128.

[7] S.-B. Park, "Profusion2 final report," PReVENT Consortium 2006, Deliverable D15.12, 2007.

[8] K. Fuerstenberg, "Intersafe2 final report," INTERSAFE-2 Consortium, Deliverable D1.2, 2011.

[9] R. Hoeger, "Haveit final report," HAVEit Consortium, Deliverable D61.1, 2011.

[10] U. Scheunert, P. Lindner, E. Richter, T. Tatschke, D. Schestauber, E. Fuchs, and G. Wanielik, "Early and multi level fusion for reliable automotive safety systems," in *Proc. IEEE Intelligent Vehicles Symp*, 2007, pp. 196–201.

[11] M. Haberjahn and M. Junghans, "Vehicle environment detection by a combined low and mid level fusion of a laser scanner and stereo vision," in *Proc. 14th International IEEE Conference on Intelligent Transportation Systems*, Washington DC, USA, 5.-7. Oct. 2011.

[12] K. Frstenberg and K. Dietmayer, "Fahrzeugumfelderfassung mit mehrzeiligen laserscannern," *Technisches Messen*, vol. 3, pp. 164–172, 2004.

[13] M. Haberjahn, "Low-level-fusion eines laserscanner- und stereokamera-systems in der fahrzeugumfelderfassung," in *Proc. of 3D-Nordost*, no. 13, Berlin, 9-10 December 2010, pp. 35–44.

[14] R. Spangenberg and T. Dring, "Evaluation of object tracking in traffic scenes," in *Proceedings of the ISPRS Commission V Symposium on Image Engineering and Vision Metrology*, Dresden, Germany, 2006.

[15] J. Manyika and H. Durrant-Whyte, *Data Fusion and Sensor Management: A Decentralized Information-Theoretic Approach*. Upper Saddle River, NJ, USA: Prentice Hall PTR, 1995.

[16] S. Mori, W. H. Barker, C.-Y. Chong, and K.-C. Chang, "Track association and track fusion with nondeterministic target dynamics," vol. 38, no. 2, pp. 659–668, 2002.

[17] C. Y. Chong, S. Mori, W. H. Barker, and K. C. Chang, "Architectures and algorithms for track association and fusion," in *IEEE AES Syst. Mag.*, 2000, pp. 5 –13.

[18] D. Franken and A. Hupper, "Improved fast covariance intersection for distributed data fusion," in *Proc. 8th Int Information Fusion Conf*, vol. 1, 2005.

[19] C.-Y. Chong, K.-C. Chang, and S. Mori, "Distributed tracking in distributed sensor networks," in *Proc. American Control Conf*, 1986, pp. 1863–1868.

[20] M. Haberjahn, "Multilevel datenfusion konkurrierender sensoren in der fahrzeugumfelderfassung," Ph.D. dissertation, Humboldt-Universitt zu Berlin, 2013, unpublished.